FRACTURE TOUGHNESS OF CARBON FIBER COMPOSITES CONTAINING VARIOUS FIBER SIZINGS AND A PUNCTURE SELF-HEALING THERMOPLASTIC MATRIX

Roberto J. Cano, Brian W. Grimsley, James G. Ratcliffe,
Keith L. Gordon, Joseph G. Smith Jr., and Emilie J. Siochi

NASA Langley Research Center
Hampton, VA 23681

ABSTRACT

Ongoing efforts at NASA Langley Research Center (LaRC) have resulted in the identification of several commercially available thermoplastic resin systems which self-heal after ballistic impact and through penetration. One of these resins, polybutylene graft copolymer (PBg), was selected as a matrix for processing with unsized carbon fibers to fabricate reinforced composites for further evaluation. During process development, data from thermo-physical analyses was utilized to determine a processing cycle to fabricate laminate panels, which were analyzed by photo microscopy and acid digestion. The process cycle was further optimized based on these results to fabricate panels for mechanical property characterization. The results of the processing development effort of this composite material, as well as the results of the mechanical property characterization, indicated that bonding between the fiber and PBg was not adequate. Therefore, three sizings were investigated in this work to assess their potential to improve fiber/matrix bonding compared to previously tested unsized IM7 fiber. Unidirectional prepreg was made at NASA LaRC from three sized carbon fibers and utilized to fabricate test coupons that were tested in double cantilever beam configurations to determine G_{Ic} fracture toughness.

1. INTRODUCTION

The initiation and propagation of damage ultimately results in failure of aircraft structural components. Often, impact damage is difficult to identify in-service, hence design of continuous carbon fiber reinforced polymer (CFRP) composite structure involves up to a 50% knockdown in the undamaged failure strength allowable. When damage is identified in a composite structure, the vehicle must be grounded for structural repair. This involves grinding away damaged regions and drilling holes to secure patches. Any activity disturbing the load bearing carbon fibers introduces new sites for damage initiation and accumulation, further weakening the structure [1]. Providing a polymer matrix with the ability to self-heal after impact damage is incurred, greatly improves vehicle safety by increasing the design allowable or strength, resulting in a more efficient CFRP structure. Self-healing polymeric materials have been defined in the literature as “materials which have the built-in capability to substantially recover their load transferring

ability after damage. Such recovery can occur autonomously or be activated after an application of a specific stimulus (e.g. heat, radiation)" [2]. Effective self-healing requires that these materials heal quickly, while retaining structural integrity. Although there are materials known to possess this characteristic, such is not the case for structural, engineering systems. In the present work, an amorphous thermoplastic has been identified that self-heals at ~50°C after through penetration by a 224 mm diameter bullet at 900 m/sec.

1.1 Self-Healing Composites State-of-the-Art

Self-healing thermoset polymeric materials are reported in the literature to mitigate incipient damage and have built-in capability to substantially recover structural load transferring ability after damage. In recent years, researchers have studied different self-healing mechanisms in materials as a collection of irreversible thermodynamic paths, where the path sequences ultimately lead to crack closure or resealing. Crack repair in polymers using thermal and solvent processes, where the healing process is triggered with heating or with a solvent, has been studied [3]. A second approach involves the autonomic healing concept, where healing is accomplished by dispersing a microencapsulated healing agent and a catalytic chemical trigger within an epoxy resin to repair or bond crack faces and mitigate further crack propagation [4]. A related approach, the microvascular concept, utilizes brittle hollow glass fibers in contrast to microcapsules filled with epoxy hardener and uncured resin in alternating layers [5-8]. An approaching crack ruptures a hollow glass fiber, releasing healing agent into the crack plane through capillary action. A third approach utilizes a polymer that can reversibly re-establish its broken bonds at the molecular level by either thermal activation (e.g., based on Diels-Alder rebonding), or ultraviolet light [9-11].

Various chemistries have been investigated based on the approaches described above. The polymer self-healing approaches found in the literature have the following disadvantages:
1) slow rates of healing, 2) use of foreign inserts in the polymer matrix that may have detrimental effects on pristine composite performance, 3) samples have to be held in intimate contact or under load and/or fused together under high temperature for long periods of time, and/or 4) not considered a structural, load bearing material even in the pristine state. For example, a self-healing composite that possesses aerospace quality consolidation with fiber volume fraction (FVF)≈60% and void volume fraction (VVF) < 2% does not currently exist [12]. Most self-healing composite laminates that have been reported possess 20-30% fiber volume that results in CFRP composites with stiffness-to-weight ratios well below that required to replace aluminum in aerospace structure [13].

1.2 Advantages Offered by Composites with a Puncture-Self-Healing Polymer Matrix

Self-healing thermoplastic materials produce a matrix healing response from a change in the material's chain mobility as a function of the damage mechanism/condition involved. This type of material possesses healing capability at elevated temperatures, fast healing rates (less than 100 microseconds), and healing without the assistance of foreign inserts or fillers. Therefore, these

materials have potential as structural aerospace materials.

Structures utilizing a high velocity puncture self-healing thermoplastic matrix may provide the following advantages: 1) improved damage tolerance compared to industry state-of-the-art thermoset CFRP, 2) a route for recovery of a proportion of the pristine mechanical properties, 3) the potential to be directly substituted for conventional thermosetting matrices that do not possess self-healing characteristics, since conventional thermoset matrix composites already suffer a knockdown of up to 50% due to inherently low damage tolerance, and 4) repeated healing from multiple damage events as long as there is no loss of matrix material incurred in the event.

Neat resin plaques of the amorphous thermoplastic PBg, shown in Figure 1, have been demonstrated to self-heal at ~50°C after through penetration by a 224 mm projectile. A CFRP fabricated with any matrix that is penetrated by a projectile can never fully self-heal due to the presence of broken carbon fibers. However, a CFRP possessing a self-healing thermoplastic can potentially recover a significant amount of compressive strength when healed after low velocity impact.

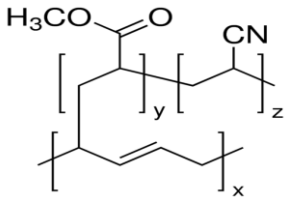

Figure 1. Chemical structure of the polybutadiene graft copolymer (PBg).

The PBg thermoplastic was selected for investigation as a matrix in CFRP experimental composites due to its higher mechanical and thermal properties compared to the other self-healing thermoplastics that have been studied. According to material suppliers, PBg has a glass transition temperature (T_g) of 80ºC, room temperature (RT) tensile strength of 37 MPa, RT tensile modulus of 2.47 GPa, and a 7.5% elongation at break [14]. The tensile modulus of the neat polymer is ~10% lower than the 2.76 GPa required of matrix polymers typically used in aerospace primary structural applications [15].

1.3 Previous Results from PBg Polymer Matrix/ Carbon Fiber Composites

Unsized IM7 carbon fiber /PBg CFRP composites have been successfully fabricated by consolidating laminates made using solution processed prepreg. Several experimental batches of IM7/PBg prepreg were produced at NASA LaRC. Based on thermal and rheological characterization of the prepreg material, a process cycle was developed to fabricate panels up to 30.5 cm x 30.5 cm. Optical microscopy (Figure 2) and acid digestion analysis of a small population of these panels revealed favorable consolidation quality, fiber volume fraction of >60% and average void volume fractions of <2%. Several $[45/0/-45/90]_{4S}$ laminates were

fabricated from both of the LaRC IM7/PBg experimental batches of prepreg and utilized to characterize the compression after impact (CAI) strength of the IM7/PBg CFRP. IM7/PBg coupons with barely visible impact damage (BVID) were subjected to a non-autonomic healing cycle at elevated temperature/pressure, similar in heat and pressure magnitude to the developed composite processing cycle. C-scan of these coupons both before and after the healing cycle indicated that the delaminations at the impact site had been healed or, at least, were no longer visible. Compression testing of these healed coupons demonstrated significant improvement in retention of strength compared to coupons having BVID. These preliminary results suggested the potential for using PBg in structural composites to mitigate low velocity impact damage following optimization of the fiber/matrix interface. [16]

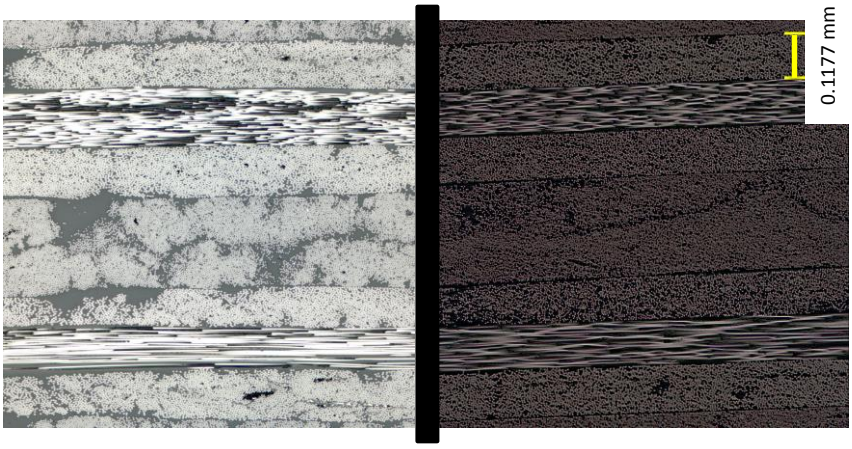

Figure 2. Optical micrographs at 100X of (A) IM7/PBg and (B) commercial IM7/977-3. [16]

All of the coupons failed due to fiber micro-buckling. In the BVID coupons, this failure initiated at the site of the impact damage and propagated across the width of the coupons. The IM7/PBg coupons containing BVID that were subjected to an elevated temperature/pressure healing cycle also failed due to fiber micro-buckling; initiating at the original impact site and propagating across the 10.2 cm width of the coupons. The pristine compressive strength resulting from the limited sample of coupons of quasi-isotropic laminates was approximately 52% of the compressive strength of the 675 MPa reported for a typical toughened epoxy 32-ply quasi-isotropic CFRP intended for aerospace structure. The fiber/matrix interface was not optimized with a fiber sizing which are typically used to optimize the interfacial adhesion in toughened epoxy CFRPs. [16] Evaluating compatible fiber sizing was the focus of this study with the goal to improve the mechanical performance of the carbon fiber/PBg composites. Therefore, several sizings were investigated in this work to assess their potential to improve the matrix/fiber interface compared to previously tested unsized IM7 fiber. Unidirectional prepreg was made at NASA LaRC from three sized carbon fibers and utilized to fabricate test coupons that were tested in double cantilever beam configurations to determine G_{Ic} fracture toughness.

2. EXPERIMENTAL

2.1 Materials

Thermoplastic polybutadiene-g-poly(methylacrylate-co-acrylonotrile) (PBg) pellets were obtained from Sigma- Aldrich® and dissolved in N-methyl-2-pyrrolidone (NMP) to afford a 31% solids solution utilized to fabricate unidirectional prepreg. The Brookfield viscosity of the resultant solution at 25ºC was determined to be 21.12 Pa∗sec (211.20 poise).

IM7-12K unsized fiber tow (Hexcel Corporation, Salt Lake City, UT, USA) was coated with a NASA LaRC identified 2% (w/v) silane solution sizing (dipodal silane {Bis[3-(Triethoxysilyl)Propyl]-Disulfide} available from Gelest Inc., Morrisville, PA, USA) at Omnia Products, Raleigh, NC, USA. Unsized fiber supplied to Omnia by NASA LaRC was sized and returned to NASA LaRC where it was re-spooled to provide the adequate number of ends to fabricate unidirectional prepreg.

Tenax®-A PCS112200 24k carbon fiber sized with XP9002 and Tenax®-A PCS122600 carbon fiber sized with U201 and PKHW-35, 50% each, was obtained from Toho Tenax America, Inc., Rockwood, TN, USA. Both sized fibers were re-spooled at NASA LaRC to provide the adequate number of ends to fabricate unidirectional prepreg.

2.2 PBg Tape Fabrication

The NASA LaRC prepregger [17] shown schematically in Figures 3 and 4 has the capability of prepregging uni-tape from resin solution, films and powders. Utilizing this prepregger, the PBg solution was used to coat the three sized fibers described in Section 2.1 to fabricate unidirectional tape. The properties of the resultant prepregs are presented in Table 1.

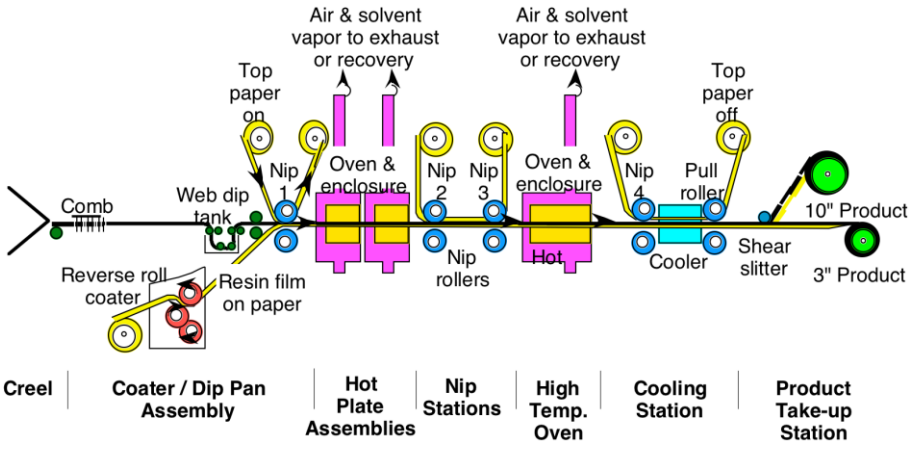

Figure 3. Schematic of LaRC multipurpose prepreg machine.

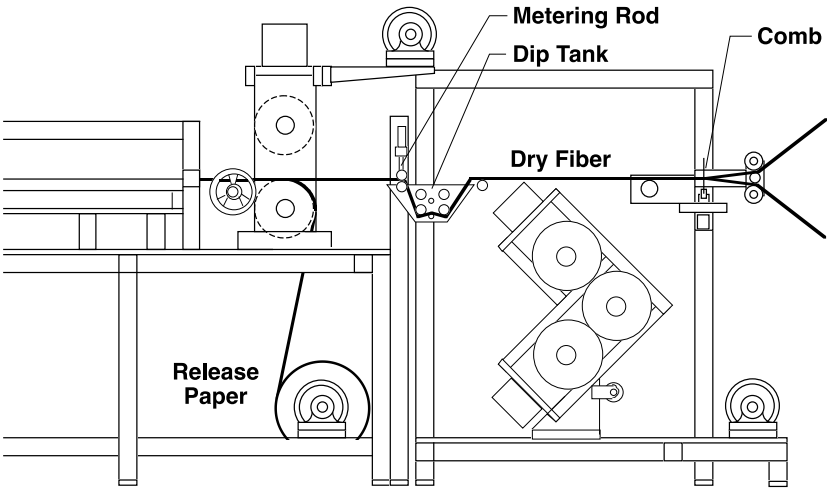

Figure 4. Schematic of solution coating.

Table 1. PBg unidirectial prepreg characteristics.

Fiber/ Sizing	Fiber Areal Weight, g/m^2	Volatiles, wt% (wet)	Resin, wt% (dry)	Length, m	Width, cm
IM7/ Unsized	154	12	38	113	21
Tenax/ XP9002	146	12	25	43	11
Tenax/ U201 & PKHW-35, 50% each	145	14	31	30	9
IM7/ LaRC Silane Sizing	135	10	35	73	9

2.3 Composite Processing

Material from each prepreg batch was processed in stainless steel closed molds using a TMP® 3 ton vacuum press with a layer of breather and release cloth separating the stack of prepreg from the stainless steel mold base and plunger. The material was processed utilizing the cure cycle developed in Reference 16 which utilized a hold at 150°C under full vacuum for 60 minutes followed by a 60 minute hold at 225°C and 1.7 MPa compaction pressure.

2.4 Mode I Fracture Toughness Double Cantilever Beam (DCB) Testing

Multiple $[0]_{32}$ carbon fiber/PBg DCB coupons were fabricated from the materials described in Section 2.2. A 12.5 mm thick Teflon crack starter was located at the center of the laminate stack extending from one machined end of the coupon 7.62 cm into the coupon and across the coupon width according to recommendations in ASTM D5528 [18]. IM7/8552 16 ply unidirectional composite panels were secondarily bonded to each surface of each PBg panel to reduce panel bending issues identified in initial DCB testing of PBg composite panels. Prior to testing, 2.54 cm piano hinges were bonded to the top and bottom plies of the DCB coupons following methods described in Reference 19. The test setup is shown in Figure 5. All DCB coupons were tested at RT using an MTS-858 table-top servo-hydraulic test frame with a calibrated 2250 N load cell. After statically pre-cracking each coupon, the piano hinges were loaded in tension under displacement control at a rate of 1.27 mm/min until the crack propagated 40 mm. The fracture toughness, G_{Ic}, was calculated using Simple Beam Theory (SBT):

$$G_{Ic} = \frac{3P\delta}{2ba}$$

and Modified Beam Theory (MBT):

$$G_{Ic} = \frac{3P\delta}{2b(a+\Delta)}$$

where, the crack extension or delamination length, a (mm), was recorded at approximately every millimeter of stable crack growth in addition to the corresponding applied load, P (N), and the load-point displacement, δ (mm). The term Δ is the delamination length correction factor determined by a least squares linear fit of the observed delamination lengths, a, versus the cube root of the corresponding compliance [18-19].

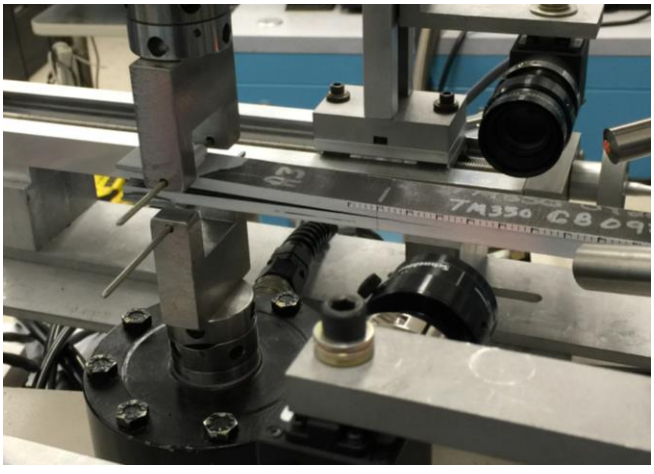

Figure 5. Photograph of DCB test setup and typical test coupon**.** (tick marks = 1 mm)

3. RESULTS AND DISCUSSION

DCB testing was performed to determine G_{Ic} fracture toughness. Typical force versus displacement curves are shown in Figures 6 and 7. The extensive fiber bridging observed during the testing (Figure 8) due to the diffuse fracturing within the composite material resulted in the need for large correction factors to be used both in the compliance calibration (CC) and modified beam theory (MBT) data reduction methods. Typical MBT G_{Ic} results for each fiber sizing are shown in Figures 9-12. This likely skewed the initiation toughness values (as no such bridging was present at this point) and therefore CC and MBT likely yield overly conservative initiation toughness values. The choice of Pc=PNL (Pc is the critical force at delamination growth initiation calculated from the load and displacement at the point of deviation from linearity, or onset of nonlinearity (NL)) did not correspond to visual observation of delamination growth as observed on the specimen edges and therefore, likely yielded an underestimate of initiation toughness. A Pc of P5% (calculated by determining the intersection of the load-deflection curve, once it has become nonlinear, with a line drawn from the origin and offset by a 5 % increase in compliance from the original linear region of the load-displacement curve) more closely corresponded to when delamination initiation was visually observed in the specimen edges and therefore, should yield fracture toughness values that correspond to growth initiation from the Teflon inserts. Based on these observations, the most appropriate initiation toughness value was determined from the SBT data reduction method with Pc=P5%. G_{Ic} increased significantly with delamination growth, which was a consequence of the diffuse fracturing. As shown in Figure 9-12, G_{Ic} was not found to plateau, which indicated that steady-state fracture was not achieved during the tests. G_{Ic} computed using the two types of specimen compliance yielded comparable (within 5%) results. This implied that although the two compliance types differ, their derivative, dC/da, did not exhibit the same difference, yielding the close comparison in toughness values. Values of G_{Ic} from the areas method compared well with those from MBT at smaller amounts of delamination extension of less than 2.54 cm (1 inch). The differences between the G_{Ic} from areas method and MBT at higher crack lengths were likely due to the increasing diffusion in fracture as delamination extension continued.

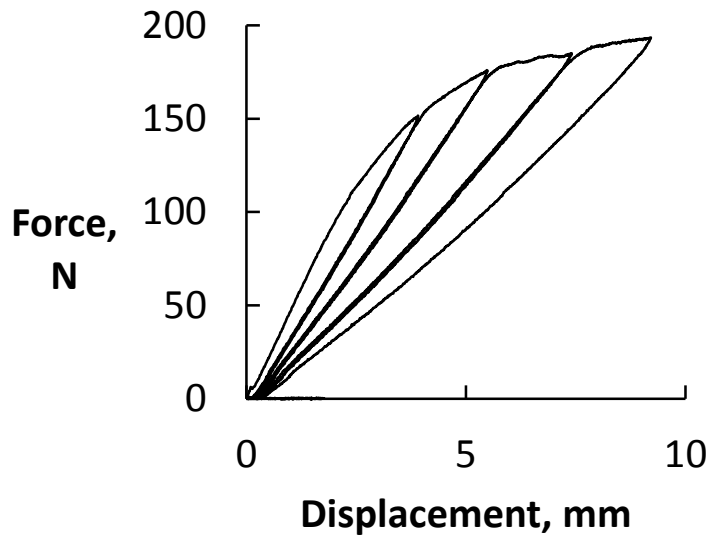

Figure 6. Typical force versus displacement curves for PBg / sized fiber samples. (PBg / Tenax, XP9002 sized fiber)

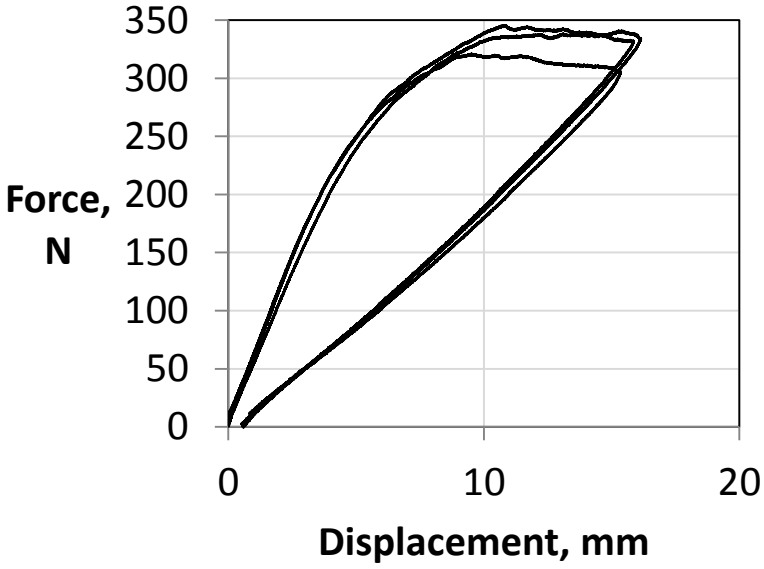

Figure 7. Typical force versus displacement curve for PBg/ unsized IM7 fiber samples.

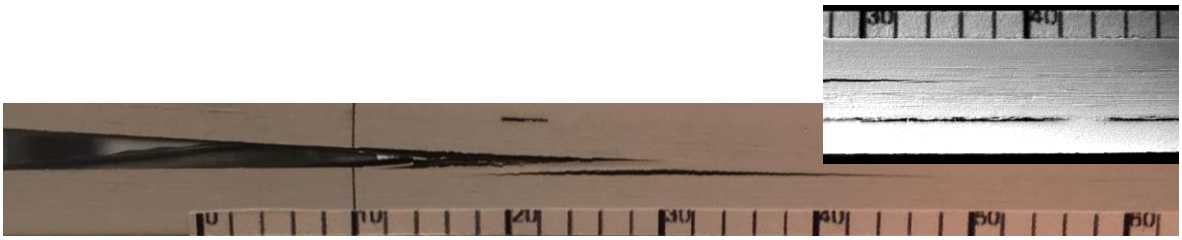

Figure 8. Photographs of typical PBg composite crack propagation. (tick marks = 1 mm)

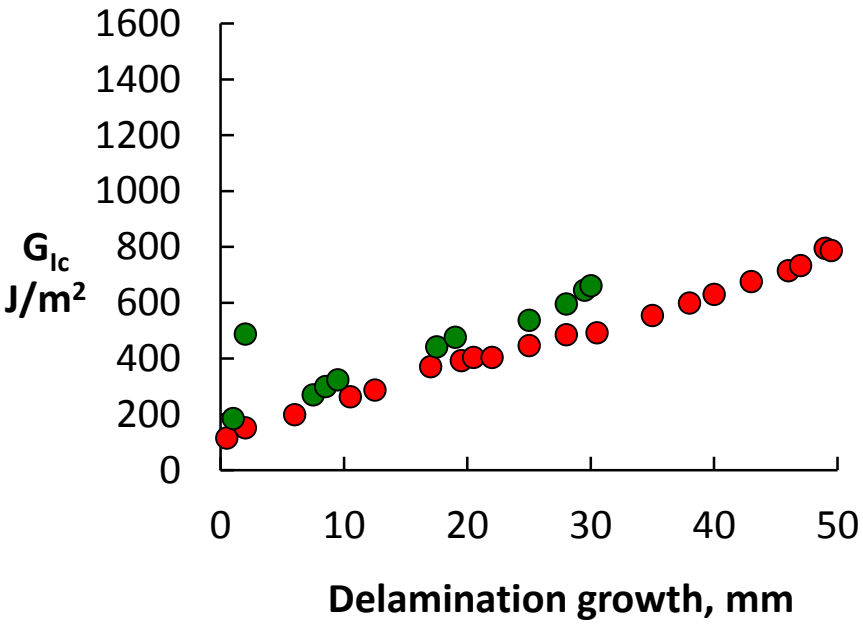

Figure 9. Typical MBT DCB data from two specimens from a PBg / Tenax, XP9002 sized fiber panel.

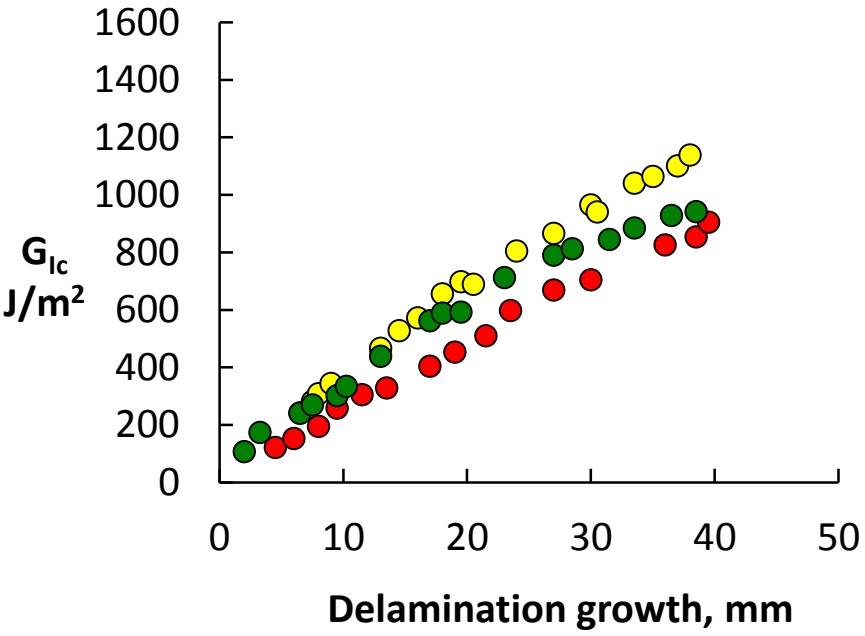

Figure 10. Typical MBT DCB data from three specimens from a PBg / Tenax, U201 & PKHW-35, 50% each, sized fiber panel.

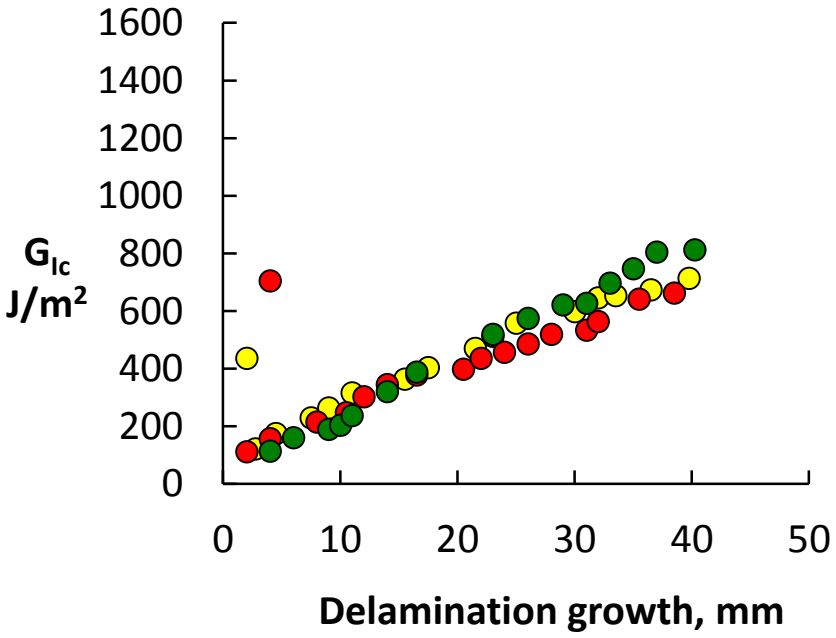

Figure 11. Typical MBT DCB data from three specimens from a PBg / IM7/ LaRC Silane Sizing sized fiber panel.

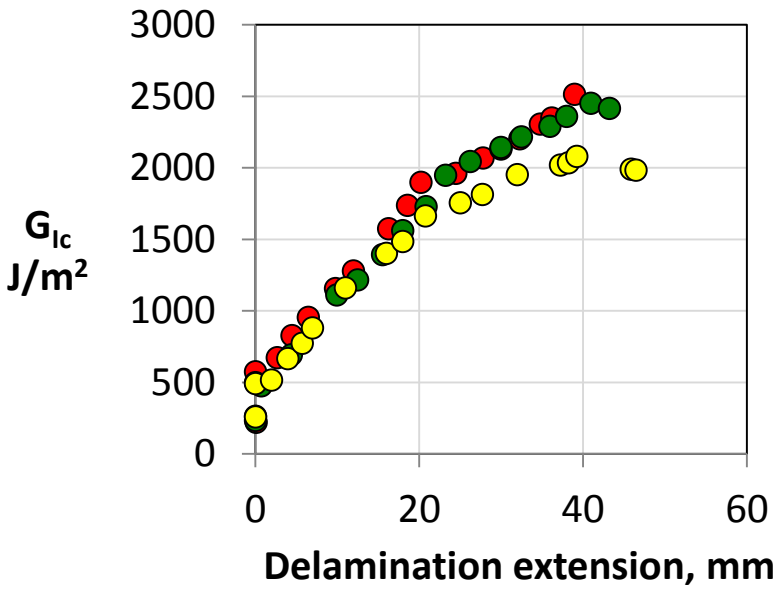

Figure 12. Typical MBT DCB data from three specimens from a PBg / unsized IM7 fiber panel.

Low-magnification edge-views of the crack growth (Figure 8) indicated that the PBg material did not appear to be as well consolidated as typical thermoset commercial systems. This was reflected in the extremely diffuse delamination growth exhibited by all specimens and arises in a rapid increase in apparent G_{Ic} as delamination growth takes place. This observation needs to be balanced by the likelihood that these materials exhibited relatively low compressive strengths due to experimental panel quality and inherent resin properties. This may counter any positive effects of the observed high resistance to delamination propagation. The specimen responses were moderately nonlinear. Consequently, all toughness values will exhibit an undefined amount of uncertainty due to the assumption of linear behavior in the data reduction methods used to calculate G_{Ic}. This is with the exception of the areas method which, however, does not yield initiation toughness values, providing only an 'averaged' sense of G_{Ic} over the corresponding delamination growth increment. The values of propagation toughness using the MBT method was generally lower than those based on compliance calibration. Therefore, only the data from MBT are reported in this paper. The toughness values from the areas method was comparable (less than 5% difference) with those from MBT at lower delamination lengths of less than 2.54 cm (1 inch). Also, the observed scatter in propagation G_{Ic} based on MBT between specimens indicated variability in the extent of fiber bridging exhibited by each specimen and therefore may indicate variation in consolidation within each panel.

The initiation fracture toughness values, G_{Ic}, of the sized and unsized fiber composites evaluated in this work are presented in Table 2 using Pc=PNL and Pc=P5%, with both the SBT and MBT methods. Panels fabricated with unsized IM7 fiber demonstrated G_{Ic} values that were significantly higher than any of the sized fiber samples. Averaged values for multiple panels

showed that the G_{Ic} values for the sized fibers were 60-67% lower for the Tenax/ XP9002 sized fiber, 53-57% lower for the Tenax/ U201 & PKHW-35, 50% each sized fiber and 69-72% lower for the IM7/ LaRC Silane Sizing sized fiber compared to the unsized IM7 fiber. Therefore, all three of the sizings evaluated in this study reduced the fracture toughness of the PBg composite in comparison with unsized IM7 fiber. Overall, the delamination initiation fracture toughness of the three sized fiber composites was moderate in value and lower than that exhibited by IM7/8552, value of 0.237 kJ/m^2 (1.35 in-lb/in^2) calculated by the MBT method as reported by Czabaj [19] for $[0]_{32}$ IM7/8552. The delamination initiation fracture toughness of the unsized IM7/PBg composite was determined to be higher than that of IM7/ 8552. However, it was not as high as those reported for the engineering thermoplastic poly(ether-ether-ketone), PEEK. A G_{Ic} of 1.7 kJ/m^2 (9.7 in-lb/in^2) is reported by Cytec [20] and a G_{Ic} between 1.3 kJ/m^2 (7.4 in-lb/in^2) and 1.44 kJ/m^2 (8.3 in-lb/in^2), depending on the type of crack initiator, by O'Brian [21] for PEEK/ AS4 composites. Cytec reports a G_{Ic} value of 2.3 kJ/m^2 (13 in-lb/in^2) for PEEK/ IM7 composites [20].

Table 2. PBg unidirectial composite G_{Ic} results.

		Initiation Fracture Toughness Values (kJ/m^2)			
Fiber/ Sizing	**Panel**	**G_{Ic} MBT PNL**	**G_{Ic} MBT P5%**	**G_{Ic} SBT PNL**	**G_{Ic} SBT P5%**
Tenax/ XP9002	**A**	**0.103**	**0.170**	**0.145**	**0.239**
Tenax/ U201 & PKHW-35, 50% each	A	0.111	0.201	0.194	0.350
	B	0.115	0.190	0.189	0.312
Average:		**0.113**	**0.195**	**0.191**	**0.331**
IM7/ LaRC Silane Sizing	A	0.071	0.123	0.117	0.205
	B	0.087	0.141	0.147	0.238
Average:		**0.079**	**0.132**	**0.132**	**0.221**
IM7/ Unsized	A	0.253	0.522	0.374	0.772
	B	0.273	0.405	0.440	0.654
Average:		**0.263**	**0.464**	**0.407**	**0.713**

Note: Averages are of six coupons from two panels. (three coupons per panel)

4. CONCLUSIONS

Three sizings were investigated in this work to assess their potential to improve the matrix/fiber interface compared to previously tested unsized IM7 fiber. Unidirectional prepreg was successfully made at NASA LaRC from three sized carbon fibers and utilized to fabricate test coupons that were tested in DCB configurations to determine G_{Ic} fracture toughness. The G_{Ic} values for the sized fibers were 60-67% lower for the Tenax/XP9002 sized fiber, 53-57% lower for the Tenax/U201 & PKHW-35, 50% each sized fiber and 69-72% lower for the IM7/ LaRC Silane sized fiber compared to the unsized IM7 fiber. All three of the sizings evaluated in this study reduced the fracture toughness of the PBg composite and did not demonstrate a potential for improvement of the mechanical properties of PBg composites.

5. REFERENCES

1. Kelly, L.G, "Composite Structure Repair," AGARD Report No 716, AFRL, Wright Patterson Air Force Base, 1983.
2. Wu, D.Y., Muere, S., and D. Solomon, "Self-Healing Polymeric Materials: A Review of Recent Developments," Progress in Polymer Science, 2008, 35, 479-522.
3. Wool, R.P., Polymer Interfaces: Structure and Strength (Hanser/Gardner, Munich, 1995)
4. White, S.R., Sotto, N.R., Geubelle, P.H., Moore, J.S., Kessler, M.R., Sriram, S.R., Brown, E.N., Viswanathan, S., Nature, 2001, 409, 794-797.
5. Pang, J.W., Bond, I.P, Composites Part A: Applied Science and Manufacturing, 2005, 36(2), 183-188.
6. Pang, J.W., Bond, I.P., Composites Science and Technology, 2005, 65 (11-12), 1791-1799.7.
7. Dry, C., Int. J Mod Phys B, 1992; 6(15-16), 2763-2771.
8. Dry, C., McMillan W., Smart Mater Struct, 1996, 5(3), 297-300.
9. John, M., Li, G., Smart Mater Struct, 2010, 19,075013-075024.
10. Nji, J., Li, G., Smart Mater Struct, 2010, 19, 035007-035015.
11. Chen, X., Dam, M., Ono, K., Mal, A., Shen, H., Nutt, S., Hera, Science, 2002, 295, 1698-1702.
12. Varley, R.J., van der Zwaag, S., Polym Int, 2010, 59, 1031–1038.
13. Smith, J. G., Jr., "An Assessment of Self-Healing Fiber Reinforced Composites," NASA TM-2012-217325, (2012).
14. Supplier Website: http://www.ineosbarex.com/files/upload/Barex210Film_07_11.pdf
15. St. Clair, T.L., Johnston, N.J., and Baucom, R.M., "High Performance Composites Research at NASA Langley," NASA TM 100518, 1988.
16. Grimsley, Brian W., Gordon, Keith L., Czabaj, Michael W, Cano, Roberto J., and Siochi, Emilie J., "Process Development of Continuous Carbon Fiber Composites Containing Puncture Self-Healing Thermoplastic Matrix", SAMPE International Symposium 2012, Baltimore, MD United States, 05/21/2012 - 05/24/2012.

17. Cano, Roberto J, Johnston, N. J. and Marchello, J:, 40th SAMPE Symposium and Exhibition, Anaheim, CA, May, 1995.
18. ASTM D5528; "Standard Test Method for Mode I Interlaminar Fracture Toughness of Unidirectional Fiber Reinforced Polymer Matrix Composites", ASTM International, 100 Barr Harbor Dr., West Conshohocken, PA, 2007.
19. Czabaj, M.W., Ratcliffe, J.R., "Comparison of Intralaminar and Interlaminar Mode I Fracture Toughnesses of a Unidirectional IM7/8552 Carbon/Epoxy Composite", *Composite Science and Technology*, Vol. 89, pp.15-23, 2013.
20. Cytec Engineered Materials Technical Data Sheet, 'APC-2 PEEK Thermoplastic Polymer', AECM-00040, Rev: 0, March 19, 2012, www.cytec.com.
21. O'Brien, T. K., and Martin, R. H., "Results of ASTM Round Robin Testing for Mode I Interlaminar Fracture Toughness of Composite Materials", *Journal of Composites Technology and Research*, Vol 15, No. 4, Winter 1993.